Transport Schemes for Unstructured Icosahedral Grids

Bill Skamarock - NCAR

Max Menchaca - NCAR/SOARS

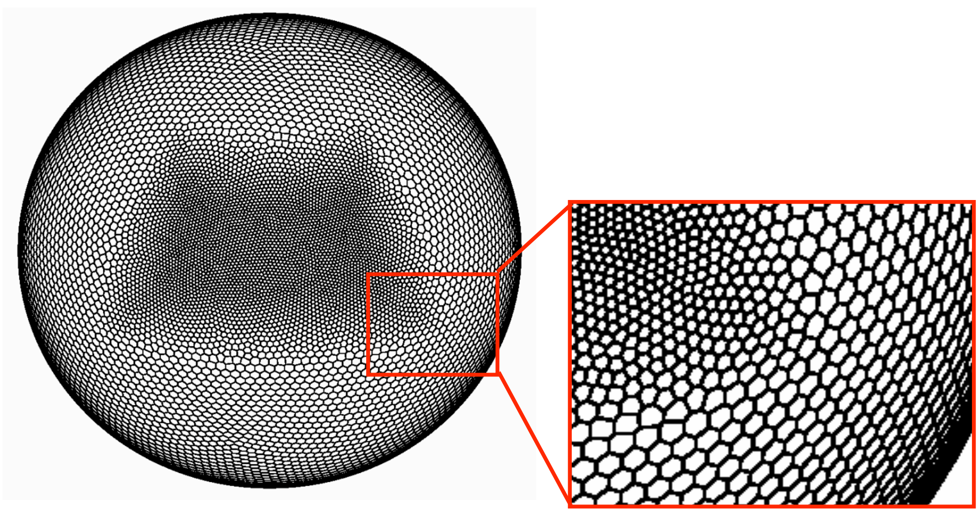

SCVTs
Spherical Centroidal Voronoi
Tessellations

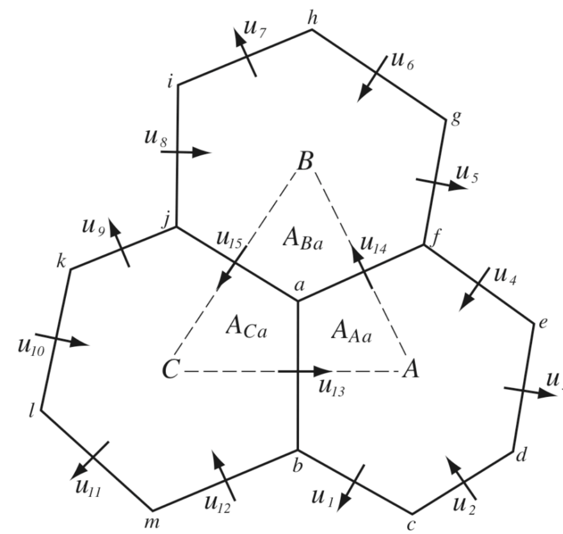

Cell center is cell center-of-mass

Edges of dual grid intersect edges of primary grid at right angles.

Unstructured-Grid Preliminaries

$$\frac{\partial(\rho\phi)}{\partial t} = -\nabla \cdot \mathbf{V}\rho\phi$$

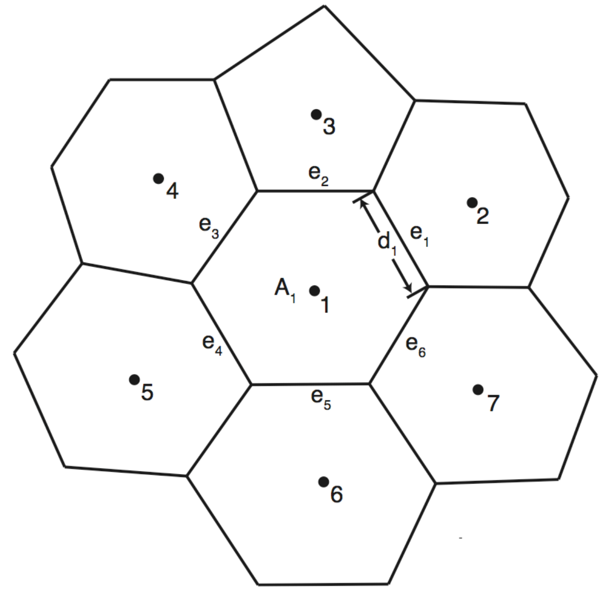

(1) Use flux (conservative) form.
(2) Require exact scalar mass conservation in the discretization.
(3) Require consistency with the mass conservation equation.
(4) Require positive-definite and monotonic options.
(5) Require a discretization for arbitrary SCVT grids - cells with *n* sides (*n* = 5, 6, 7, … sides).

Continuous ⟹ Discrete Equations

$$\frac{\partial(\rho\phi)}{\partial t} = -\nabla \cdot \mathbf{V}\rho\phi$$

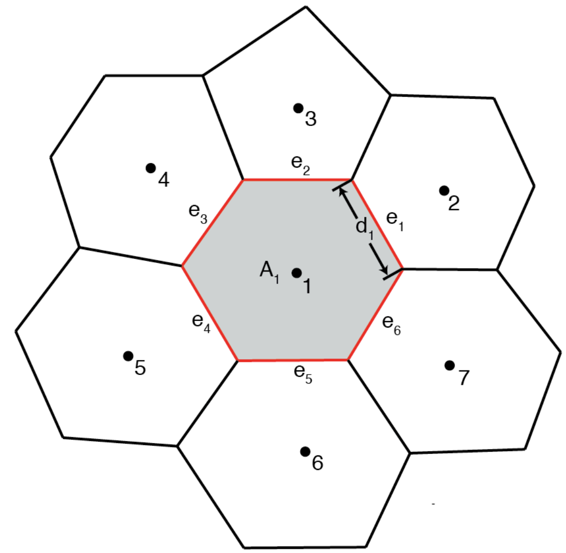

Forward-in-time
Finite volume discretization

$$\int\int \frac{\partial\rho\phi}{\partial t}\, dA\, dt \;=\; -\int\int \nabla\cdot \mathrm{V}\rho\phi\, dA\, dt$$

Integrate space and time

$$A\,\frac{(\overline{\rho\phi})^{t+\Delta t} - (\overline{\rho\phi})^{t}}{\Delta t} = -\int\left(\int (\rho\phi\, u\cdot\vec{n})\, d\Gamma\right) dt$$

Use divergence theorem

$$\left[(\overline{\rho\phi})^{t+\Delta t} - (\overline{\rho\phi})^{t}\right]_i = -\frac{1}{A_i}\sum_{n_e} d_{e_i}\, (\rho u_\perp \phi \Delta t)\,|_{e_i}$$

Apply to cell

Discretizations

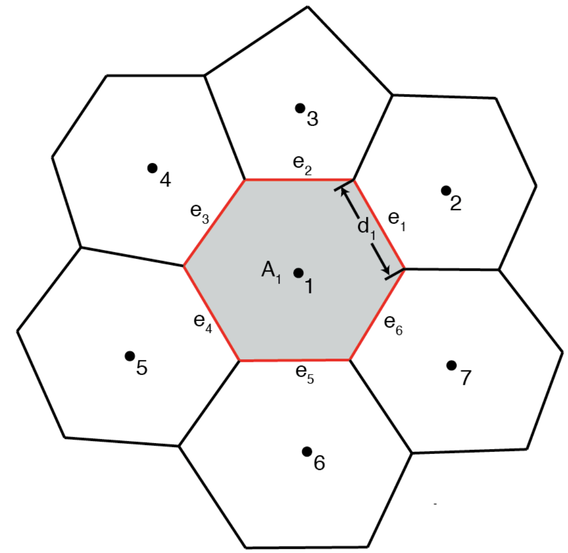

$$\left[(\overline{\rho\phi})^{t+\Delta t} - (\overline{\rho\phi})^{t}\right]_i = -\frac{1}{A_i}\sum_{n_e} d_{e_i}\,(\rho u_\perp \phi \Delta t)\,|_{e_i}$$

Conservative if the same flux is used to update both cells sharing an edge (e.g $(d_1 \rho u_\perp \phi)_1$ is used to update $(\overline{\rho\phi})_1$ and $(\overline{\rho\phi})_2$).

Consistent if $$\left[(\overline{\rho})^{t+\Delta t} - (\overline{\rho})^{t}\right]_i = -\frac{1}{A_i}\sum_{n_e} d_{e_i}\,(\rho u_\perp \Delta t)\,|_{e_i}$$

Formulation allows for a variety of PD and monotonic limiters.

How can we compute $(d_1 \rho u_\perp \phi)_1$?

Discretizations

Possibilities for $(d_1 \rho u_\perp \phi)_1$ ($(u_\perp)_1$ is directed out of cell 1)

(1) 1st order upwind: $(d_1 \rho u_\perp \phi)_1 = (du_\perp)_{e_1} \cdot (\overline{\rho\phi})_1$

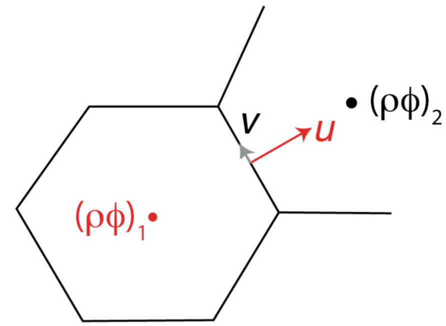

Monotonic
Unacceptably dissipative

(2) 2nd order ~ centered:

$$(d_1 \rho u_\perp \phi)_1 = (du_\perp)_{e_1} \cdot \frac{1}{2}\left[(\overline{\rho\phi})_1 + (\overline{\rho\phi})_2\right]$$

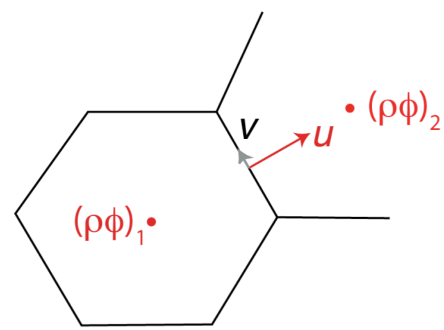

Less than 2nd order on irregular grids.
Unstable for FIT integration (can use LF, RK, AB, other schemes)
Can be monotonized within some time-integration schemes.

Discretizations

(3) Incremental remapping (Lipscomb and Ringler, 2005; Yeh, 2007)

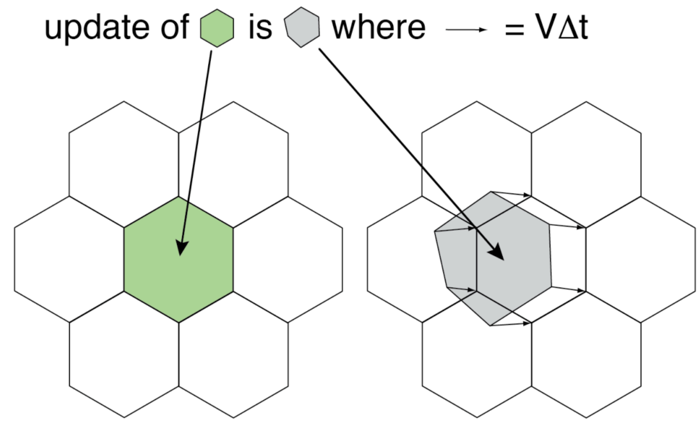

Remapping (departure cell to arrival cell)

Incremental remapping (departure cell to arrival cell)

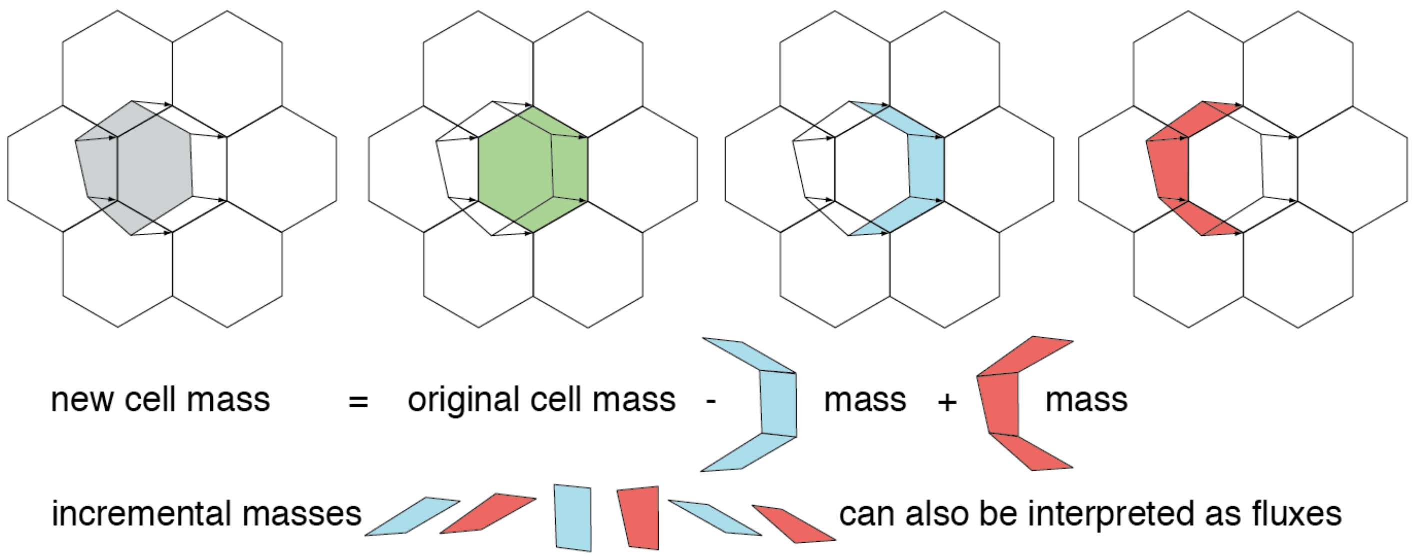

Discretizations

(3) Incremental remapping (Lipscomb and Ringler, 2005; Yeh, 2007)

1st order polynomial specifies scalar distribution.

$$\phi(x,y) = \phi_1 + c_1 x + c_2 y$$
$$= \phi_1 + \phi_x x + \phi_y y$$

ϕ_x and ϕ_y are computed as an average of those computed by fitting planes to values at the vertices of the triangles of the dual grid.

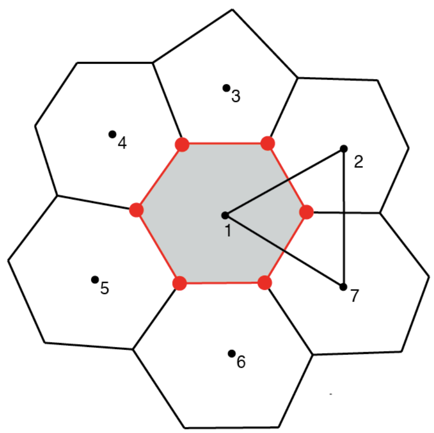

Quadrature requires evaluation of the polynomial at the centroid of the triangles comprising the scalar mass flux.

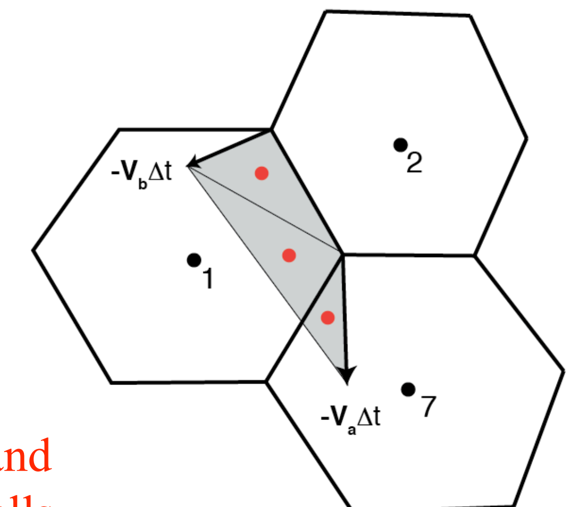

Determination of the quadrature points is complex, costly, and often requires performing quadrature over many different cells for a single flux.

Discretizations

(4) Upwind-biased advection (Miura 2007)

Similar to LR (2005) and Yeh (2007) but uses the assumption that the velocity is constant along a cell edge, and uses only the upwind neighbor in the quadrature.

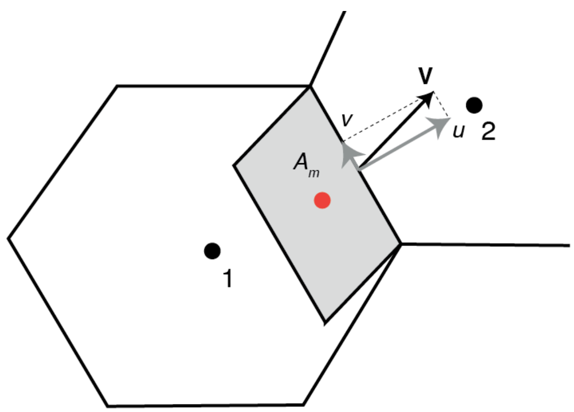

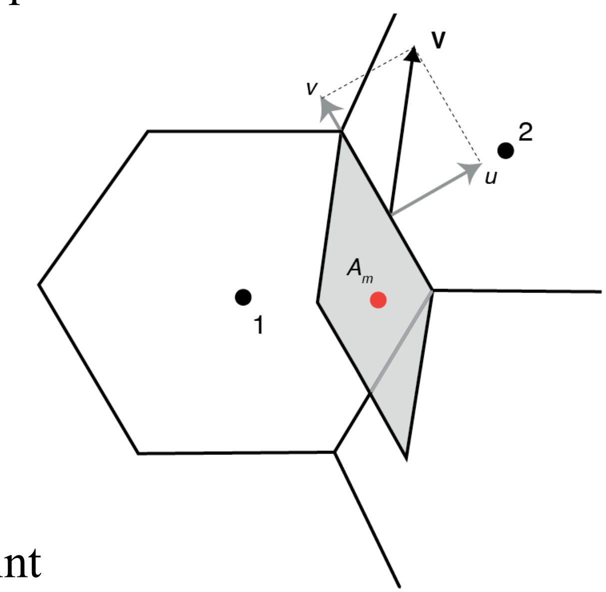

Departure region is a parallelogram, single-point quadrature is sufficient for linear polynomial. Polynomial is determined by least-squares fit to points.

Much simpler and less costly than LR (2005) and Yeh (2007), and similar in accuracy.

Discretizations

(5) Our extension of Miura (2007)

$$
\begin{aligned}
\phi(x,y) &= \phi_1 + c_1 x + c_2 y \\
&\quad + c_3 x^2 + c_4 xy + c_5 y^2 \\
&= \phi_1 + \phi_x x + \phi_y y \\
&\quad + \frac{1}{2}\left(\phi_{xx} x^2 + 2\phi_{xy} xy + \phi_{yy} y^2\right)
\end{aligned}
$$

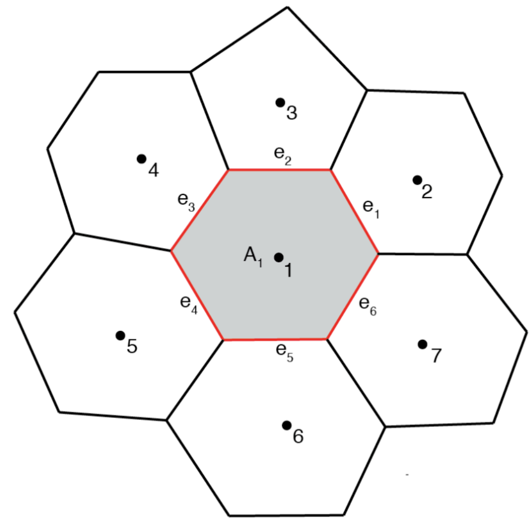

We use the *same stencil* as Miura (2007), LR (2005), Yeh (2007) for polynomial fit, but we use a *quadratic polynomial* (least-squares fit to cell-average values).

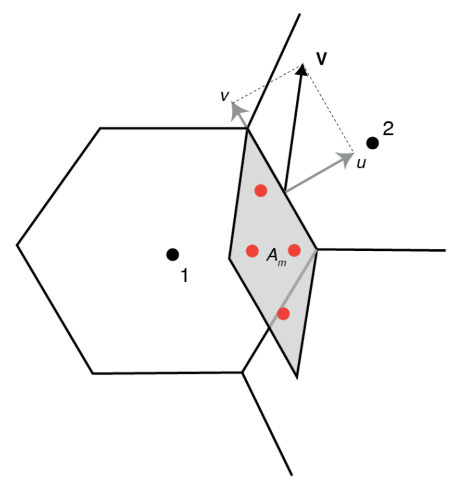

Parallelogram requires 4 evaluations of polynomial in the quadrature.

Constant term is adjusted such that the integral over the cell is equal to the cell area times the cell-averaged value.

Results

Williamson et al (JCP 1992) - Test case 1

Solid body rotation, 12 day integration to circle the sphere.
Initial and end state are identical.

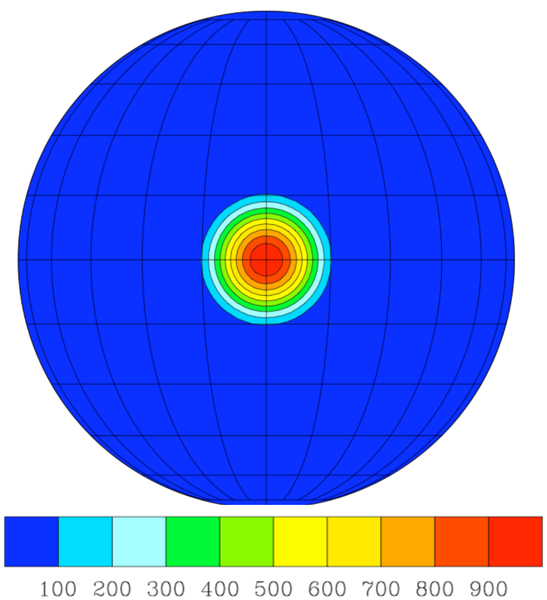

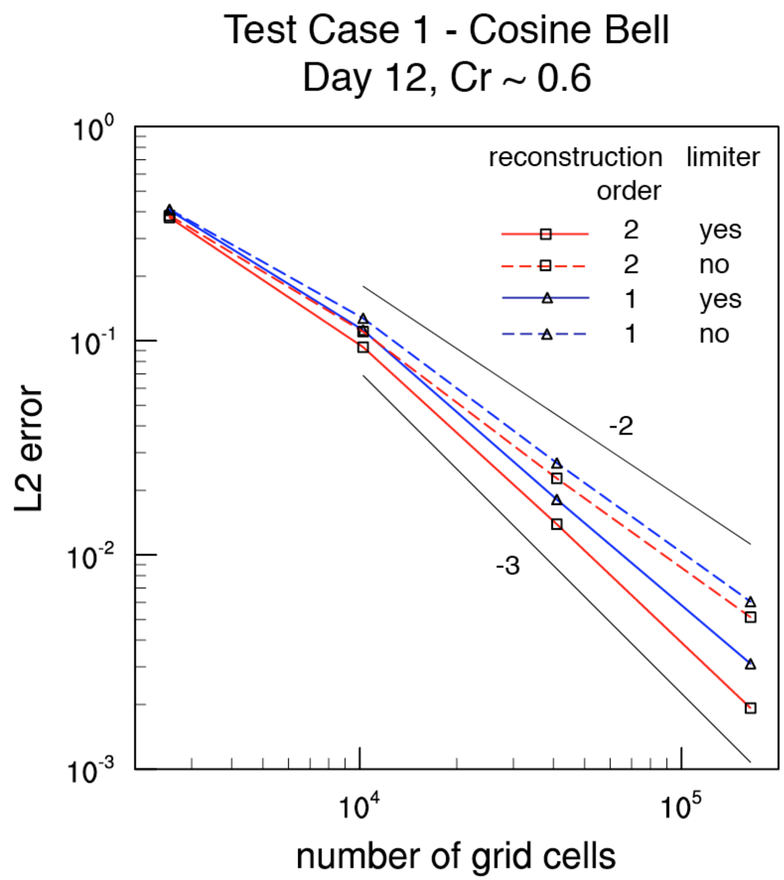

- First order reconstruction reproduces Miura.
- Use of a monotonic limiter reduces the error.
- For constant Cr=0.6, reduction of error with 2nd order reconstruction is small compared with 1st order reconstruction.

Results

For smaller Courant numbers, accuracy of 1st-order reconstruction degrades dramatically. The 2nd-order reconstruction is much less affected by the Courant number (timestep)

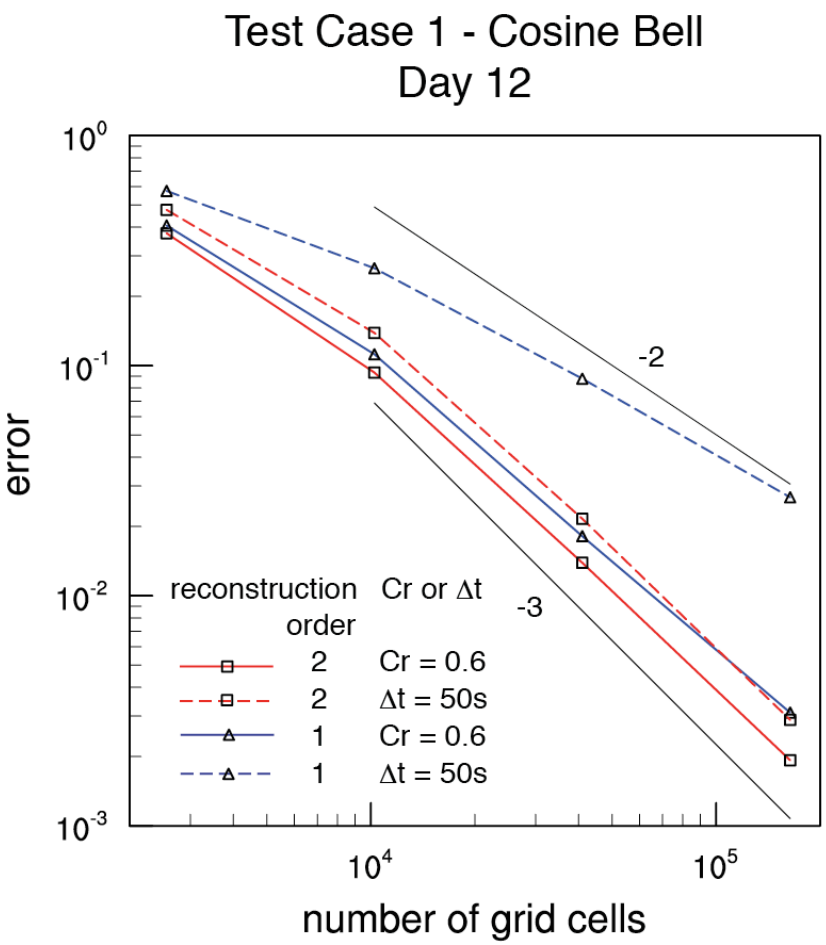

N	Δx	Δt (Cr=0.6)	Cr (Δt=50 s)
2562	480	7200 s	4×10^{-3}
10242	240	3600 s	8×10^{-3}
40962	120	1800 s	1.6×10^{-2}
163842	60	900 s	3.2×10^{-2}

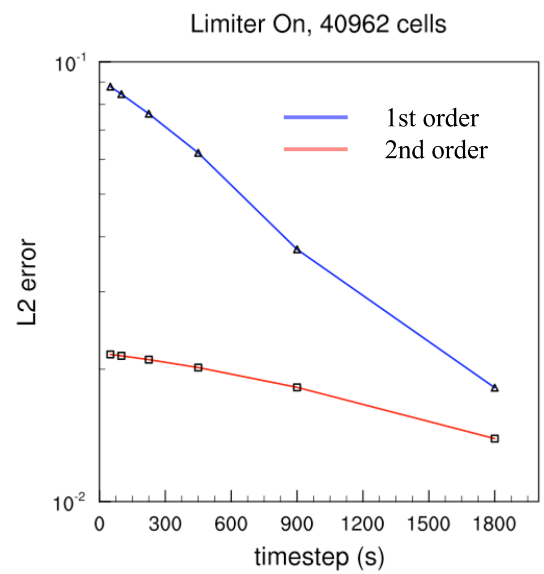

Results

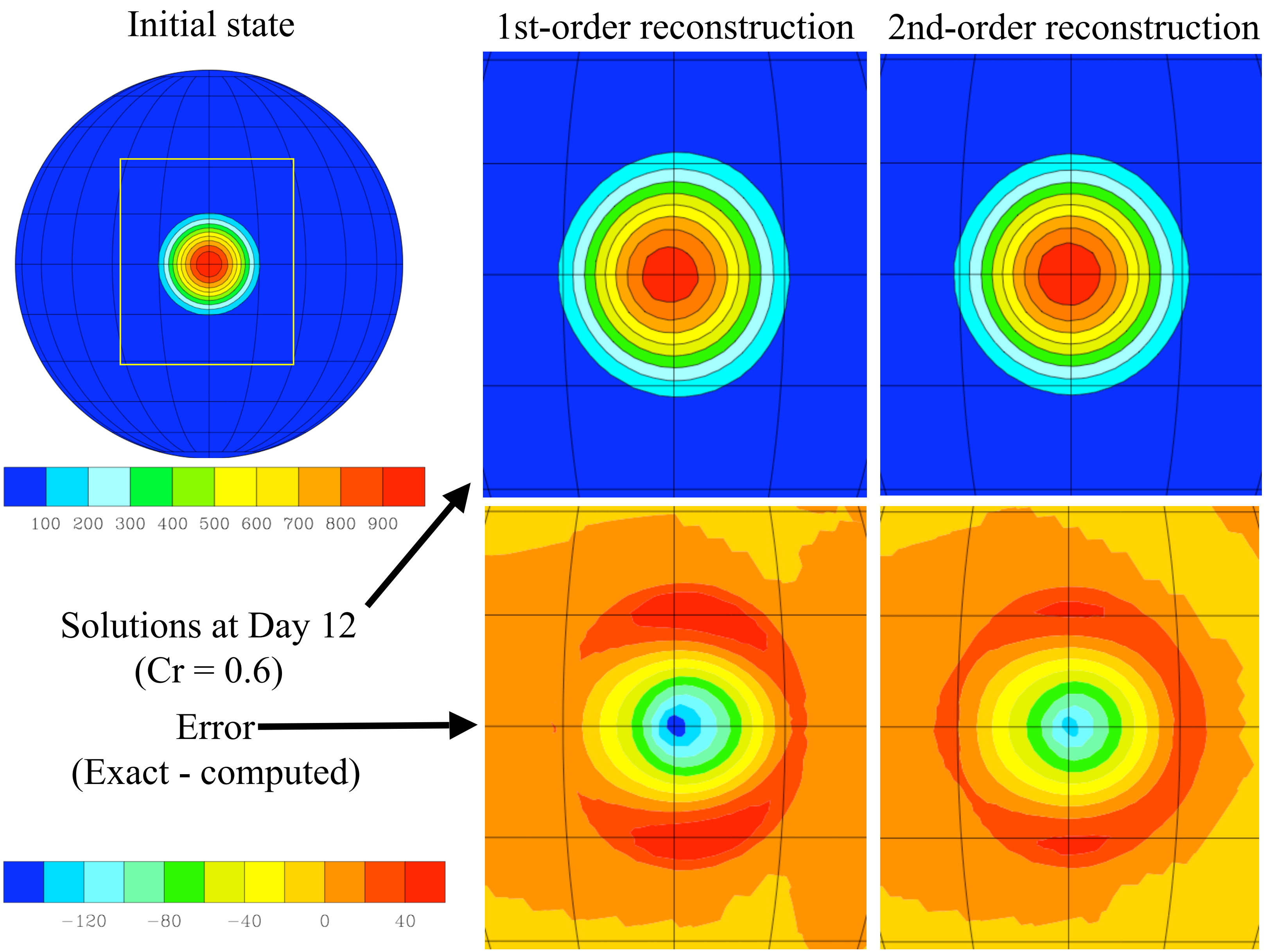
Initial state
1st-order reconstruction
2nd-order reconstruction
100 200 300 400 500 600 700 800 900
Solutions at Day 12
(Cr = 0.6)
Error
(Exact - computed)
−120 −80 −40 0 40

Results

Initial state

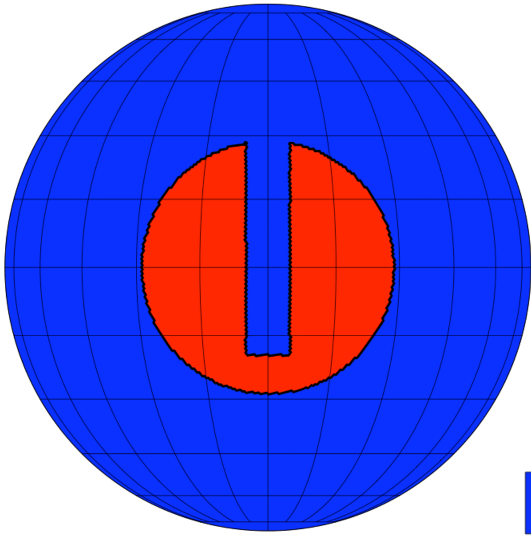

Slotted-cylinder advection - test of monotonic limiter (Zalesak 1979).

Limiter performs as expected.
Discontinuity spread over $\sim$ 5 cells.

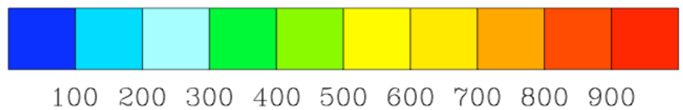

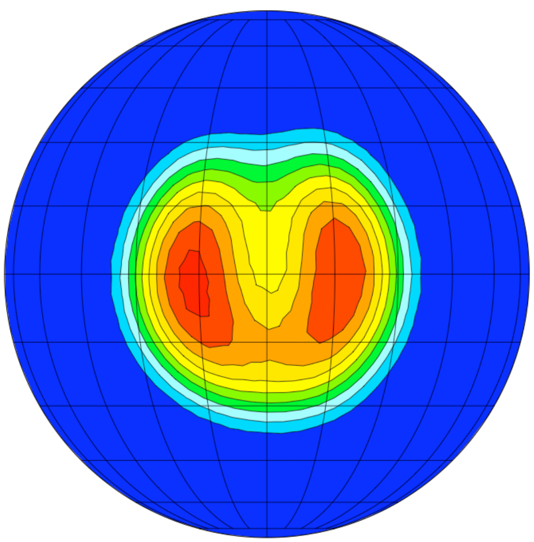

Day 12, 2562 Cells

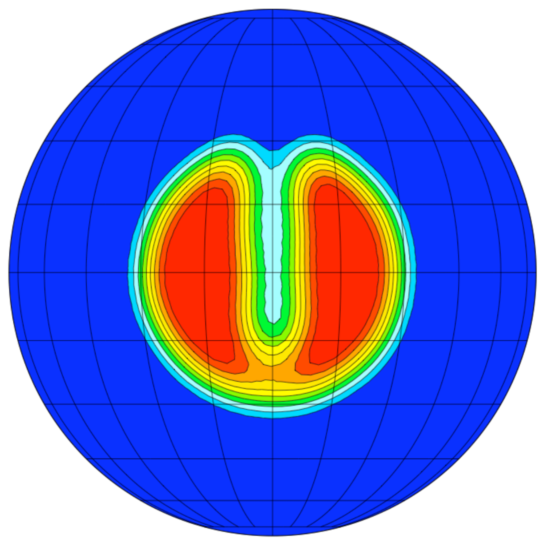

Day 12, 10242 Cells

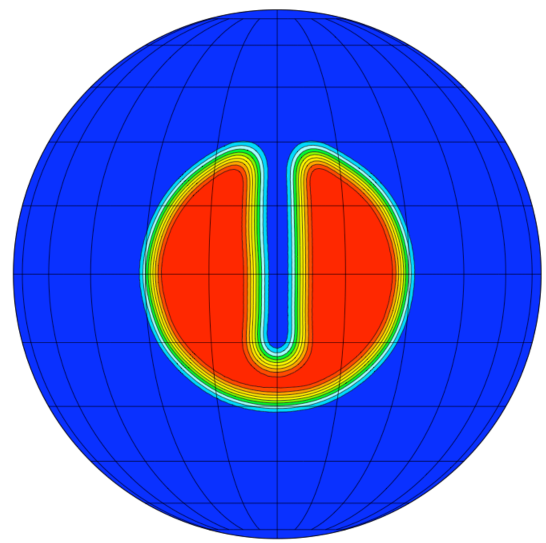

Day 12, 40962 Cells

Results

Initial state

Day 12, 10242 Cells
2nd-order reconstruction

Day 12, 10242 Cells
1st-order reconstruction

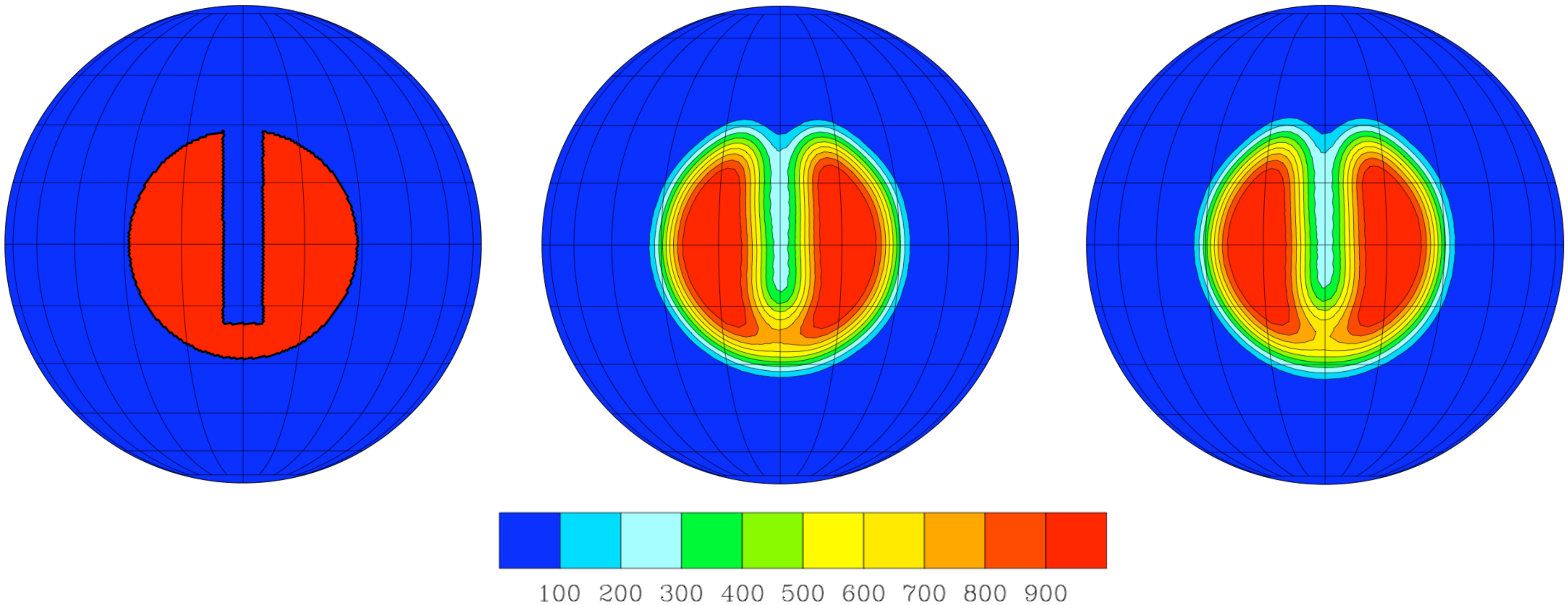

Differences between 2nd and 1st order reconstruction results are small for discontinuous features.

Results - Reconstruction

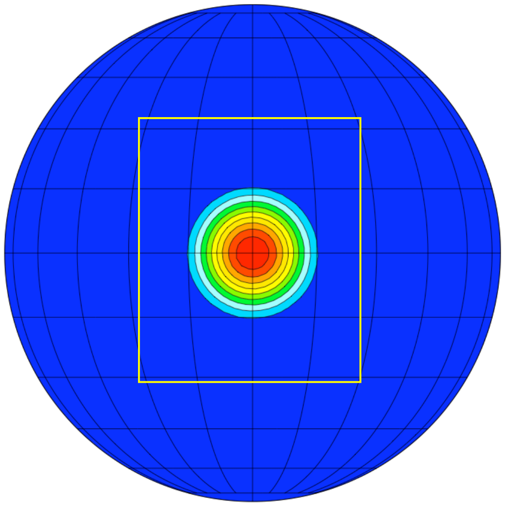

2nd order reconstruction

$$
\begin{aligned}
\phi(x,y) &= \phi_1 + c_1 x + c_2 y \\
&\qquad + c_3 x^2 + c_4 xy + c_5 y^2 \\
&= \phi_1 + \phi_x x + \phi_y y \\
&\qquad + \frac{1}{2}\left(\phi_{xx} x^2 + 2\phi_{xy} xy + \phi_{yy} y^2\right)
\end{aligned}
$$

ϕ_x

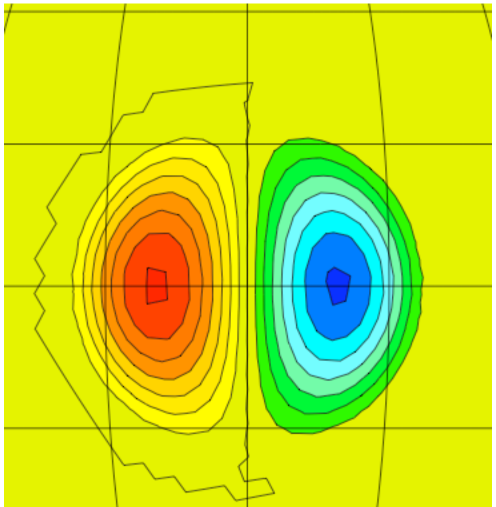

10242 Cells, initial state

ϕ_{xx}

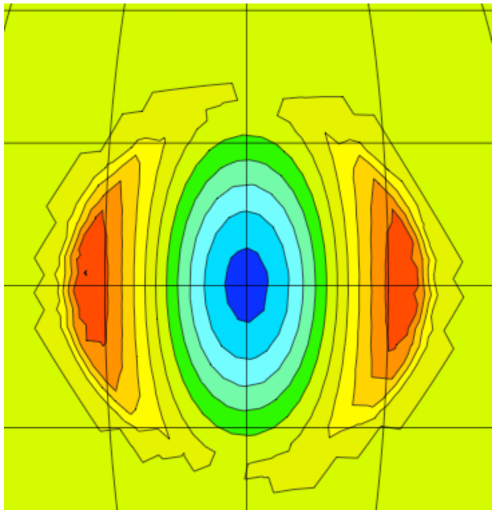

10242 Cells, initial state

ϕ_{xy}

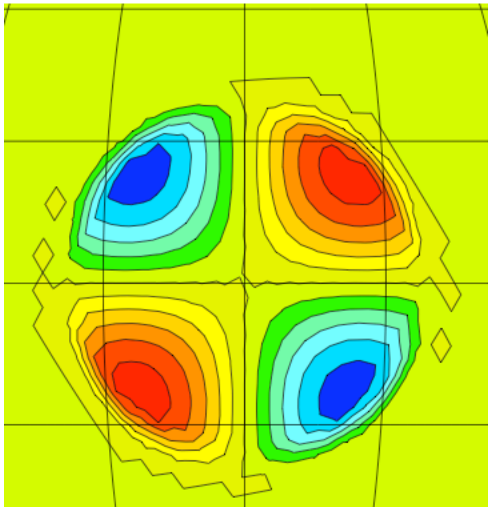

10242 Cells, initial state

Results - Reconstruction

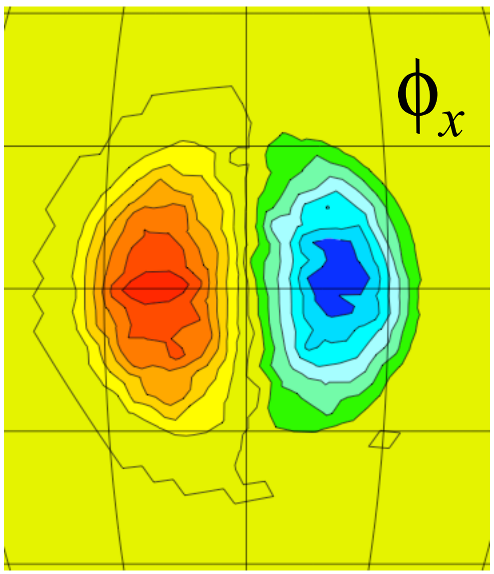

Fitting planes to the triangles on the dual grid, averaging slopes.

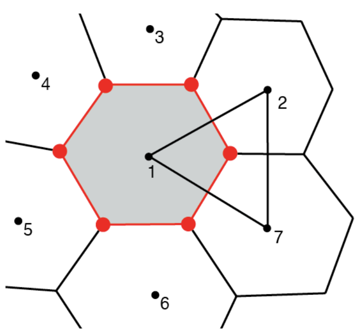

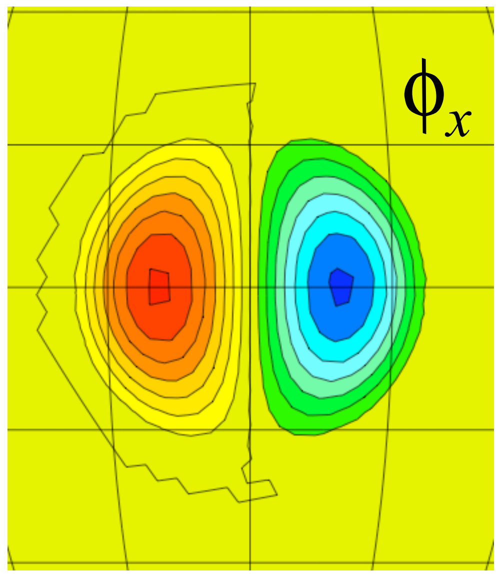

Using Green's theorem

$$\oint_C \phi \, dx = \iint_A \left(-\frac{\partial \phi}{\partial y} \right) dx \, dy$$

$$\oint_C \phi \, dy = \iint_A \left(\frac{\partial \phi}{\partial x} \right) dx \, dy$$

Computation of higher derivatives?

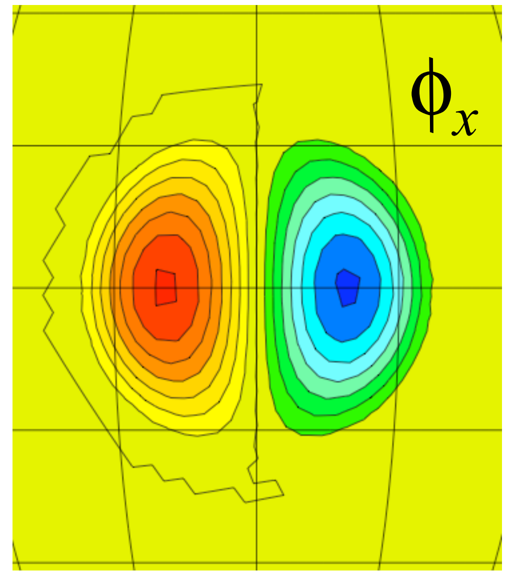

Least-squares fit

Robust. Direct computation of full polynomial.

Results - Deformational flow

Perfect hexagons on a plane (Blossey and Durran 2008)

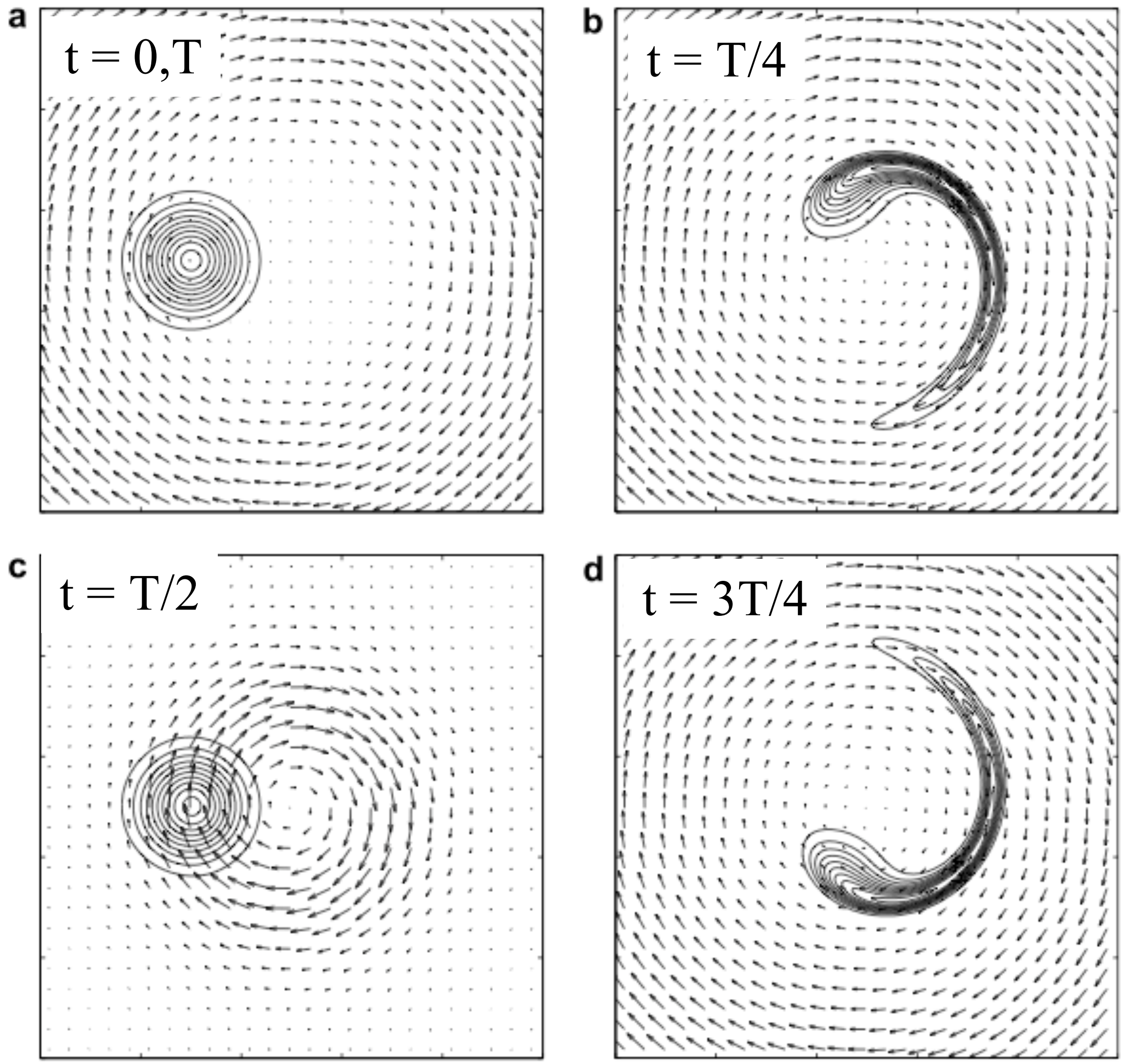

Results - Deformational flow

Perfect hexagons on a plane (Blossey and Durran 2008)

For reference:

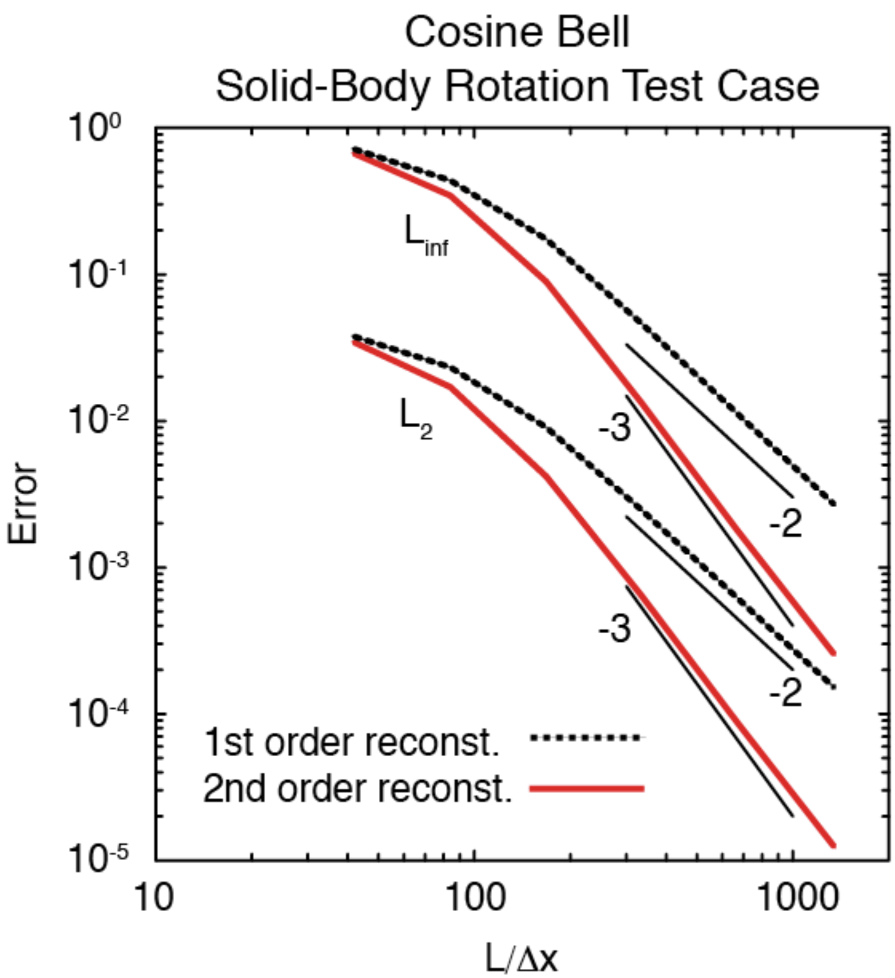

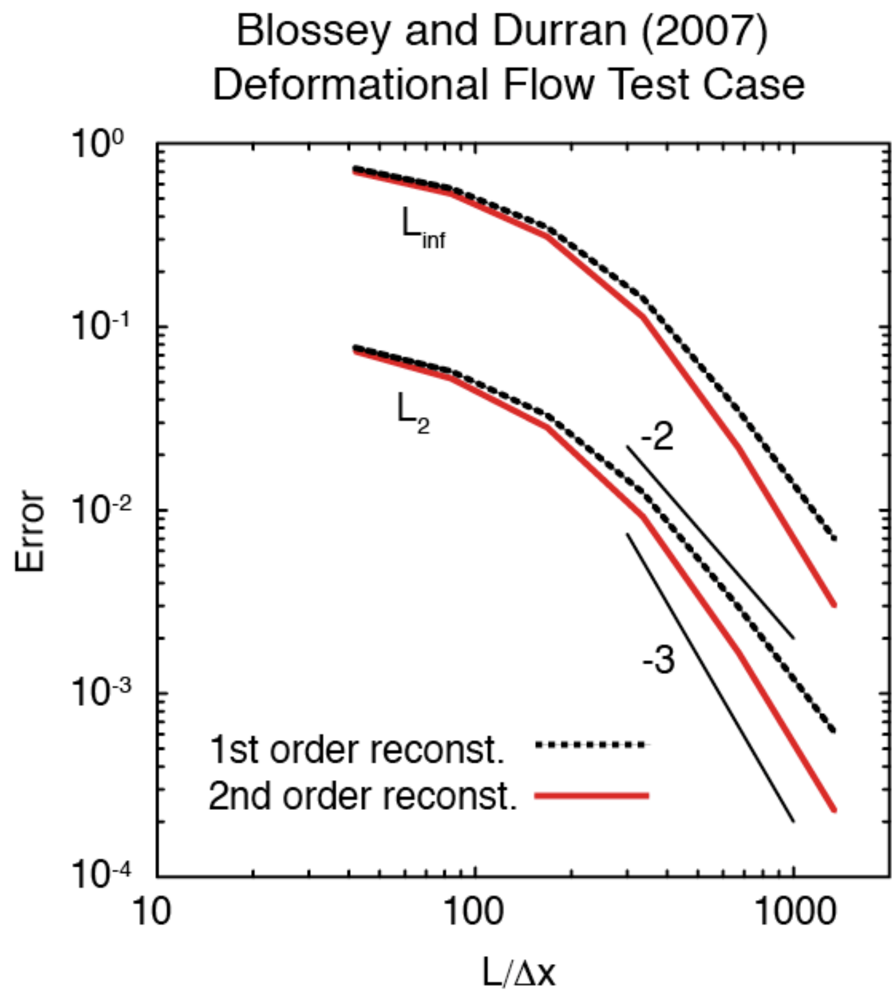

Summary

Extension to Miura (2007) transport scheme:
2nd order polynomial for cell mass reconstruction.

(1) Uses same stencil as 1st order reconstruction.

(2) More accurate than 1st-order reconstruction in all cases, has a smoother distribution or the error (e.g L_2 norms).

(3) Accuracy of 2nd-order scheme much less dependent on timestep than 1st-order scheme.

(4) Convergence rate approaches third order for smooth flows, regardless of Cr number.

(5) Successfully tested for deformational flows, discontinuous distributions (using Zalesak 1979 limiter).

Future work: role of geometric error (constant **V** assumption along cell edge) in limiting accuracy.